

SELF-ASSEMBLED MONOLAYERS AS NUCLEATING SURFACES TO  
CONTROL ACETAMINOPHEN POLYMORPHS

A Thesis

Presented to the Faculty of the Graduate School  
of Cornell University

In Partial Fulfillment of the Requirements for the Degree of  
Master of Science

by

Zihao Zhang

December 2017

© 2017 Zihao Zhang

## ABSTRACT

Polymorphism, the phenomenon in which a compound crystallizes into more than one solid state crystal structure, has drawn attention in many industry fields, especially pharmaceuticals. In recent years, self-assembled monolayers (SAMs) have been used to study polymorph control because of their well-defined surface chemistry and structure. Furthermore, by tuning the substrate-crystal interface energy, potentially SAMs can promote the nucleation of polymorphs not accessible via solution methods. These advantages have led us to choose heterogeneous surface nucleation via SAMs as the primary means to study polymorph selection. In this work, we have examined multiple SAM chemistries on gold and silicon in the presence of various solvent systems to investigate their ability to influence the nucleation, crystal growth, and polymorph selection of a common drug, acetaminophen (ACM). We have found that both solvent and substrate work together to control crystal polymorph. On hydrophobic, methyl and phenyl terminated surfaces, using water, ethanol, or dioxane as solvent results in the monoclinic polymorph, while the orthorhombic polymorph is formed when using mixtures of water and dioxane. As a comparison to hydrophobic surfaces, hydroxyl terminated surfaces were investigated. In this case, using ethanol or dioxane as solvents results in orthorhombic polymorph selection, clearly different from crystallization results on hydrophobic surfaces. Interestingly, the methyl and phenyl terminated surfaces that promote the formation of the less thermodynamically stable orthorhombic form of ACM show (002) cleavage planes perpendicular to the substrate, while the -OH terminated surfaces induce that same polymorph with the

(002) cleavage planes parallel to the substrate surface. We hypothesize that this selection is due to the energetic favorability of certain crystal facets interacting with the chemically distinct SAM surfaces.

## BIOGRAPHICAL SKETCH

Zihao was born in Daqing, a city known as the Oil Capital of China. He went to boarding school at the age of 10, which was unusual among peers and this experience cultivated the independence in his personality. He loved watching documentaries and the wonders of nature led him to the way of pursuing science study. Studying materials science and engineering guided him into better understanding the laws of physics and chemistry, and also their applications in real life.

Zihao entered Tianjin University as an undergraduate and experienced three and a half treasurable years there in the School of Materials Science and Engineering. Later, he was selected, based on academic achievements, to build up undergraduate thesis in the Ian Wark Institute of University of South Australia(UniSA). From UniSA, he worked on an environmental-related project, “Selective extraction of metal ions from complex and saline leach solution using surface modified diatomaceous earth(DE) particles”. Besides improvement of research skills, he learned to respect the work of science and engineering.

Zihao joined Prof. Ulrich Wiesner’s and Prof. Lara Estroff’s group in the Department of Materials Science and Engineering in September. 2017. His project was on using self-assembled monolayers as nucleating surfaces to study early formation pathways of crystallographic polymorphs. After graduation, he will go back to China and find a job.

## DEDICATIONS

[Dedication page is optional, has no heading, centered on page horizontally and vertically]

## ACKNOWLEDGMENTS

I would like to thank Prof. Ulrich Wiesner and Prof. Lara Estroff for giving me an opportunity to join their groups and conduct research in their labs. I also would like to thank Katherine Barteau for her training and guiding on me during the past two years. Maura Weather offered great help on my X-ray learning and I really appreciate that. Many thanks to my colleagues in both Wiesner and Estroff groups for their valuable suggestions on my research work. Lastly, this research was supported by the International Fine Particle Research Institute (IFPRI) and by the Cornell Center for Materials Research with funding from the NSF MRSEC program (DMR-1120296).

.....

## TABLE OF CONTENTS

Abstract.....	iii
Biographical Sketch.....	v
Dedication.....	vi
Acknowledgement.....	vii
List of Figures.....	ix
List of Tables.....	x
 Chapter 1. Introduction and background.....	 1
1.1 Polymorphism.....	1
1.2 Classical nucleation theory.....	3
1.2.1 Homogeneous nucleation.....	3
1.2.2 Heterogeneous nucleation.....	4
1.3 Existing methods of screening polymorphs.....	5
1.4 Self-assembled monolayers.....	7
1.4.1 Thiol-gold chemistry.....	7
1.4.2 Silane-silica chemistry.....	8
1.5 Goal.....	9
1.6 References.....	10
 Chapter 2. Self-assembled monolayers as nucleating surfaces to study crystallographic polymorphs.....	 15
2.1 Introduction.....	15
2.2 Experimental section.....	17
2.2.1 Materials.....	17
2.2.2 Thiol-gold substrate preparation.....	18
2.2.3 Silane-silica substrate preparation.....	18
2.2.4 Solution preparation.....	19
2.2.5 Crystallization.....	20
2.2.6 Characterization of ACM crystals.....	21
2.3 Results.....	22
2.3.1 Role of solvent on polymorph selectivity.....	22
2.3.2 Role of solvent and substrate on polymorph selectivity .....	25
2.3.3 Role of substrate on crystal orientation.....	27
2.3.4 Surface morphology of ACM crystals on PTS and MUOH.....	29
2.4 Discussion.....	30
2.5 Conclusion.....	34
2.6 References.....	35
 Chapter 3. Conclusion and preliminary works for future study.....	 41
3.1 Conclusion.....	41
3.2 Preliminary blade coating work.....	41

## LIST OF FIGURES

Figure 1.1 The free energy change as a function of spherical nucleus radius.....	4
Figure 1.2 Schematic of heterogeneous nucleation on a solid substrate .....	4
Figure 1.3 Schematic of an ideal, single crystalline alkanethiolate SAM formed on a (111) orientated gold substrate.....	7
Figure 1.4 Growth mechanism of OTS molecules on silica substrate under a) dry condition and b) wet condition .....	9
Figure 2.1 Acetaminophen.....	16
Figure 2.2 Crystallization set-up of droplet experiments: a) 4 droplets of ACM solution are on an UDT-covered gold coated wafer under room temperature b) Schematic of droplet experiments on SAM-modified substrate from side view .....	20
Figure 2.3 Representative XRD data of ACM Form I and Form II.....	23
Figure 2.4 XRD data of crystallization on UDT, OTS, PTS, and MUOH SAM chemistry with using mixture of water and dioxane as solvent. ....	26
Figure 2.5 2D X-ray Diffraction pattern of ACM on PTS(a) and MUOH(b) surfaces with solvent as water/dioxane mixture.....	27
Figure 2.6 SEM images of Form II surface morphology on PTS and MUOH SAMs grown from 20:80 water:dioxane. ....	29
Figure 2.7 Schematic representation of the proposed molecular interaction between Form II crystals and SAM. Form II crystallized (a) on PTS SAMs with (002) orientation and (b) MUOH SAMs with (002) orientation.....	34

## LIST OF TABLES

Table 1.1 Variation in chemical and physical properties in polymorphs.....	2
Table 2.1 Chemical structures of SAMs molecules .....	17
Table 2.1 Crystallization results on different SAM chemistries with various solvents.....	24
Table 3.1 Substrate types and solvent types for blade-coating.....	42
Table 3.2 Preliminary results of manually blade coating .....	43
Table 3.3 Preliminary results of blade coating with controlled speed.....	44

## Chapter 1. Introduction and Background

### 1.1 Polymorphism

Polymorphism is a phenomenon in which a compound crystallizes into more than one solid state crystal structure. Polymorphs of the same compound have large variations in the physico-chemical properties, such as thermodynamic stability, solubility, or dissolution rate as shown in Tab. 1.1. Polymorphism is important for applications of chemicals ranging from organic electronic materials, pigments, food ingredients (e.g., in chocolate production), and pharmaceuticals. For example, in the organic semiconductor (OSC) field, small changes among polymorphs (e.g., molecular packing) results in substantial changes in the charge transport properties.<sup>2</sup> Another example concerns the pigment industry, where there is the well-known polychromism (i.e., multiple colors) example of 5-methyl-2-[(2-nitrophenyl)amino]-3-thiophenecarbonitrile, referred to as ROY and known for its red, orange, and yellow crystals among different polymorphs.<sup>3</sup> Furthermore, ROY has seven polymorphs, the largest number recorded in the Cambridge Structural Database (CSD).<sup>4</sup>

In the development of new pharmaceuticals, bioavailability and stability are two key properties to be considered. Bioavailability is highly related to the drug solubility and dissolution rate in the human body (e.g., aqueous solutions at ~ pH 7). It has been reported that the solubility ratio between polymorphic pairs is generally less than two.<sup>5</sup> For this reason, polymorphs of the same compound can have very different bioavailabilities. For example, in 1998, a new polymorph of an anti-HIV drug, Ritonavir, appeared in the formulation vehicle. This new form was 50% less soluble

than the one, which had already been launched into the market. The difference in the solubility between the two polymorphs resulted in drastically lower dissolution and bioavailability of the new polymorph. Therefore, Ritonavir was withdrawn from the market by Abbott. As a result of stories such as this one, pharmaceutical companies are paying increasing attention to identifying polymorphs early in the production of new drug candidates, as well as developing methods for better controlling polymorph selection.

**Table 1.** Variation in chemical and physical properties in polymorphs<sup>1</sup>

<p><b>Chemical</b></p> <ul style="list-style-type: none"> <li>• Chemical reactivity/stability</li> <li>• Photochemical reactivity</li> </ul>	<p><b>Kinetic</b></p> <ul style="list-style-type: none"> <li>• Rate of dissolution</li> <li>• Solid-state reaction kinetics</li> <li>• Stability</li> <li>• Rate of crystal growth</li> </ul>	<p><b>Mechanical</b></p> <ul style="list-style-type: none"> <li>• Compactability</li> <li>• Hardness</li> <li>• Powder flow</li> <li>• Tableting</li> <li>• Tensile strength</li> </ul>
<p><b>Packing/physical</b></p> <ul style="list-style-type: none"> <li>• Conductivity</li> <li>• Density (or molar volume)</li> <li>• Hygroscopicity</li> <li>• Refractive index</li> <li>• Color</li> <li>• Particle morphology</li> </ul>	<p><b>Surface</b></p> <ul style="list-style-type: none"> <li>• Interfacial tensions</li> <li>• Surface area</li> <li>• Surface free energy</li> </ul>	<p><b>Thermodynamic</b></p> <ul style="list-style-type: none"> <li>• Chemical potential, free energy, and solubility</li> <li>• Enthalpy and entropy</li> <li>• Heat capacity</li> <li>• Melting and sublimation temperature</li> <li>• Vapor pressure</li> </ul>

There are probably a number of polymorphism-related pharmaceutical events not known to the public. Generally, clinical failures of drugs can be caused by differences in performance among polymorphs. Moreover, undesired polymorph production can result in manufacturing problems, batch rework, and delays in project or clinical timelines.<sup>1</sup> Nowadays, the question is whether it is possible to predict how many

polymorphs a specific molecule has and how to produce a desired polymorph selectively.

## **1.2 Classical nucleation theory**

Nucleation is the process of forming a new solid phase from a supersaturated mother phase and is the starting point to all types of crystallization. Classical nucleation theory (CNT) is the most common theoretical mode and can be classified into two categories: homogeneous nucleation and heterogeneous nucleation.

### **1.2.1 Homogeneous nucleation**

Homogeneous nucleation is defined as nucleation occurring in a homogeneous phase without preferential nucleation sites. In classical nucleation theory, the Gibbs free energy ( $\Delta G$ ) of the nucleation barrier is estimated by simplifying the situation into one spherical nucleus first formed in the liquid phase. In order to quantify the nucleation process, consider the radius of a spherical nucleus as  $r$ . Under this condition,  $\Delta G$  as a function of the radius of the spherical nucleus is derived as followed:

$$\Delta G(r) = \frac{4}{3}\pi r^3 \rho \Delta\mu + 4\pi r^2 \gamma \quad \text{Eq. 1}$$

$\rho$  is the density of molecules in the liquid phase,  $\Delta\mu$  is the chemical potential difference between the phase in which nucleation occurs, and the nucleation phase itself, and  $\gamma$  is the surface tension of the interface between nucleus and liquid phase.

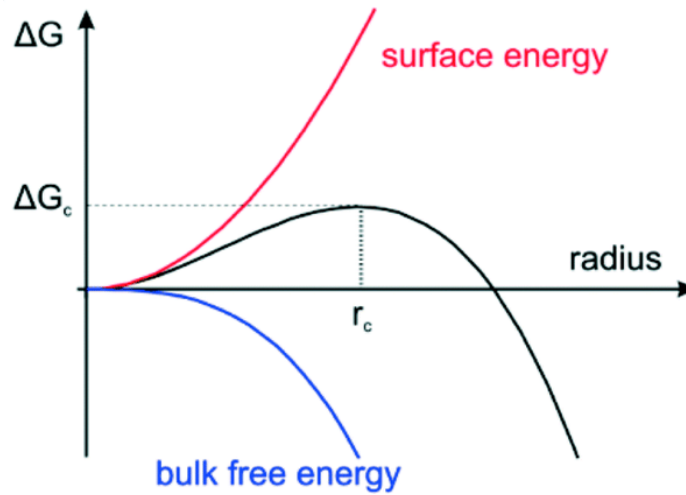


**Figure 1.** The free energy change as a function of spherical nucleus radius.<sup>6</sup>

Fig. 1 shows how the Gibbs free energy of the nucleation barrier depends on the radius of nuclei according to Eq. 1, as well as surface energy and bulk free energy contributions to the free energy. The maximum in the curve at  $r_c$  corresponds to the radius where any change of nucleus size would result in a decrease in Gibbs free energy. The corresponding size to  $r_c$  is called the critical nucleus size.

### 1.2.2 Heterogeneous nucleation

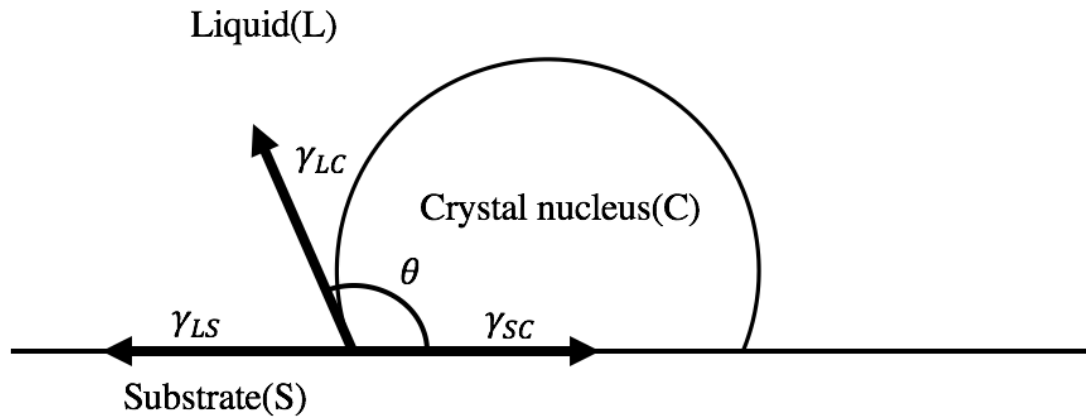


**Figure 2.** Schematic of heterogeneous nucleation on a solid substrate

Heterogeneous nucleation is defined as nucleation occurring at preferential nucleation sites and these sites, for example, can be suspended foreign particles in the liquid system. Under the assumption that the nucleus is still sphere-like in heteronucleation, the Gibbs free energy of the nucleation barrier is estimated by Eq. 2 shown below. Eq. 2 can also be divided into two parts, the volume energy contribution and the surface energy contributions. Compared to Eq. 1, the second term of Eq. 2 is more complex, now taking solvent-substrate (LS), solvent-nucleus (LC), and nucleus-substrate (SC) interfacial energies into consideration. Finally, heterogeneous nucleation is much more common than homogeneous nucleation, since induced nucleation sites always results in a lower nucleation barrier, which means a lower supersaturation level is required to nucleate.

$$\Delta G(r) = \frac{4}{3}\pi r^3 \rho \Delta \mu + S_{LC} \gamma_{LC} + (\gamma_{SC} - \gamma_{LS}) S_{SC} \quad \text{Eq. 2}$$

### 1.3 Existing methods of screening polymorphs

There are various existing experimental methods of identifying polymorphs. In industry, high through screening (HTS) methods are employed. Factors, such as cooling temperature, cooling rate, solvent type, and supersaturation level, are usually optimized in HTS to get as many polymorphs as possible. Traditionally, polymorphs are identified through time-consuming methodologies such as exhaustive screens of different solvents, cooling or evaporation rates, and supersaturation level to discover as many polymorphs as possible.<sup>7, 8</sup> It is widely recognized that the majority of crystallization events on the lab scale is the result of heteronucleation. Since crystallization theory hypothesizes that crystals grow from nuclei, intervening with

nucleation at early stages is studied to control polymorphism.<sup>9-11</sup> For example, the group of Michael Ward controlled growing glycine polymorphs in nano-scale channels of glass beads and polymer monoliths. Small molecular additives also play an important role in polymorph control.<sup>5, 12</sup> In the work of the group of Meir Lahav, by tuning the structure of small molecular additives as inhibitors, the  $\beta$  polymorph of glycine was grown in aqueous solution.<sup>13</sup> Epitaxial nucleation on single crystal substrates is also put forward to probe polymorphism, because of the almost perfect ordering surface of the single crystal.<sup>14-17</sup> In 2002, Matzger and his coworkers employed polymers with diverse functional groups as heterogeneous nucleation sites to study and control polymorphism of small organic molecules. Moreover, by varying functional groups and solvent types, this approach succeeded in controlling polymorph production of two important pharmaceuticals, acetaminophen and carbamazepine.<sup>18</sup>

Recently, several researchers have used self-assembled monolayers (SAMs) as substrates to alter the energetic barrier to the nucleation of different polymorphs. For example, Jingkang Wang and his co-workers achieved selective crystallization of tolbutamide on SAMs with methyl, trifluoromethyl, and phenyl functional groups.<sup>19</sup> Finally, the Aizenberg group demonstrated that well-defined patterned SAMs can induce nucleation of calcite polymorphs with specific orientation.<sup>20</sup> While all these results are encouraging, a comprehensive understanding of the parameters that govern polymorph selection on SAMs is still missing.

## 1.4 Self-assembled monolayers

### 1.4.1 Thiol-gold chemistry

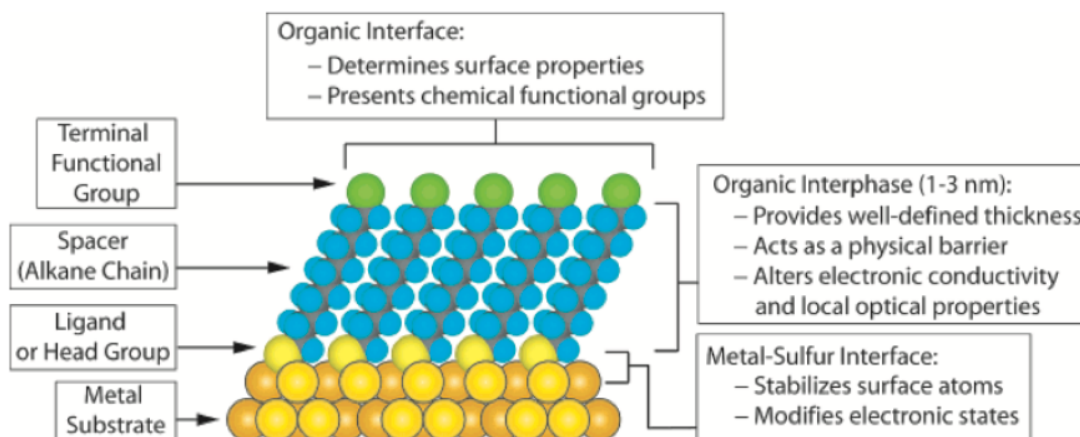


**Figure 3.** Schematic of an ideal, single crystalline alkanethiolate SAM formed on a (111) orientated gold substrate.<sup>21</sup>

Long-chain alkanethiols self-assemble to form SAMs on gold (Fig. 3). Such thiol-gold based systems are historically the most studied SAMs.<sup>22,23</sup> The four components of these SAMs are shown in Figure 3 and are (from top to bottom): terminal functional group, spacer, ligand, and metal substrate. By using various terminal chemical functional groups, different surface properties can be obtained for the study of crystallization phenomena. Well-defined thickness, usually 1~3 nm, can be varied via adjusting the number of carbons in the alkane chain. At the same time, the specific thickness of the spacer plays a role as physical barrier between terminal surfaces and underlying substrates. There are several other reasons to choose thiol-based SAMs on gold for crystallization experiments. First, gold-coated silicon wafers are commercially available. Second, gold is reasonably inert under environmental conditions, which means it does not oxidize nor react with most chemicals at room

temperature. Additionally, by manufacturing gold into a smooth and flat substrate (i.e., with low surface roughness), well-defined 2D SAMs are accessed in which the alkane spacers crystallize in 2D, thereby providing well-pack, crystalline organic layers with variable surface functionality. The affinity between gold and thiols is so high that gold does not undergo other reactions easily.<sup>21</sup> Gold-thiol SAMs are typically stable up to 14 days in tris- buffered saline (TBS) solutions at 37 °C.<sup>24</sup>

#### **1.4.2 *Silane-Silica chemistry***

In the 1980s, Chiesey studied the growth mechanism of alkylsilane SAMs and characterized the SAMs surface properties.<sup>23</sup> Silanization occurs on glass and metal oxide surfaces, whereby the reaction between substrate hydroxyl groups and silane molecules leads to the formation of covalent –Si-O-Si- bonds. Continuous efforts have been devoted to study the growth mechanisms of silane-silica SAMs and how to get to ultrasmooth SAMs. Taking SAMs grown from octadecyl-trichlorosilane (OTS) as an example, Fig. 3 shows the formation process of OTS SAMs step by step under dry and wet conditions.<sup>25,26</sup> Based on previous studies, a thin water film (several molecular layers) covering the silica substrate is essential for SAM formation, since OTS initially reacts with this water film covering the silica substrate.<sup>27</sup> Under dry conditions, i.e. with no additional water molecules in the environment, OTS molecules react with this bound water first and, then, with other OTS molecules that are attaching to the silica substrate surface. Eventually, a uniform and complete monolayer is obtained. In contrast, under wet condition, OTS molecules may react with free water molecules forming OTS-crosslinked aggregates first before hitting the substrate. Eventually,

OTS-crosslinked aggregates attach to the substrate by only a few covalent bonds, leading to a multilayer with higher roughness and thickness.

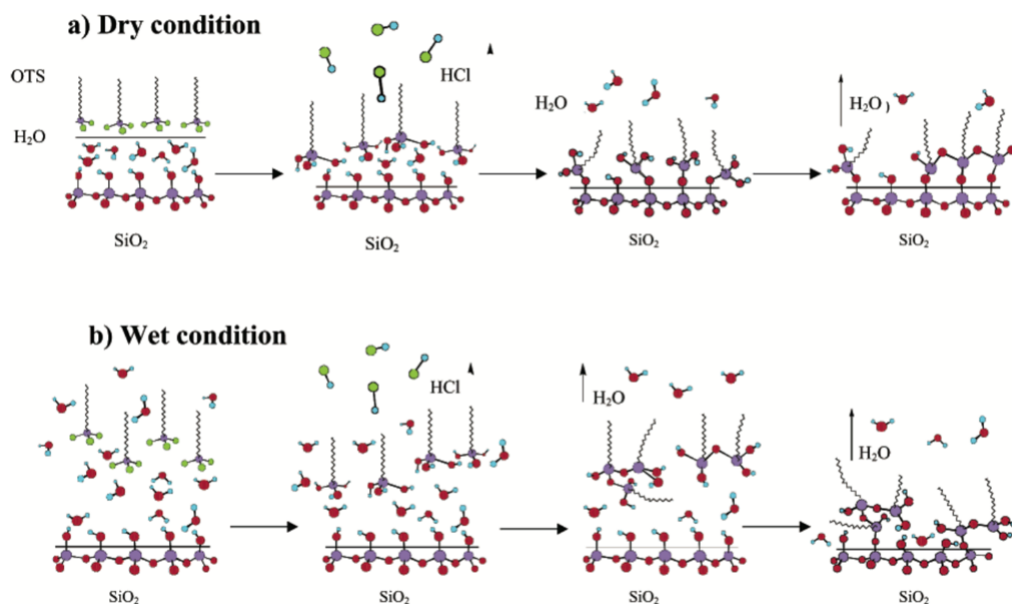


**Figure 4.** Growth mechanism of OTS molecules on silica substrate under a) dry condition and b) wet condition.<sup>26</sup>

Generally, silane-based SAMs on Si wafers, when formed under the proper conditions as described above, can show properties like high chemical homogeneity and low surface roughness. Moreover, a variety of surface chemistries can be achieved by changing the end group of the silane molecules. With respect to SAM quality, thiol-gold SAMs provide the best and most well-defined surfaces. However, silane-based SAMs are more mechanically robust and more thermally stable, up to 250 °C.<sup>28</sup> These properties altogether make thiol-alkane and silane-coated SAMs ideal choices to study polymorph selectivity.

## 1.5 Goal

Polymorphism is an important aspect that has to be considered for many different applications of materials because of large variations in properties among different polymorphs. However, it is still not clear how to best assess the existence of different polymorphs and how to control polymorph selection for a specific chemical compound. Compared to homogeneous nucleation, heterogeneous nucleation offers a higher chance to discover and control polymorphism by lowering the surface energy barrier to nucleation. Here, we chose SAMs from gold-thiol and silane chemistries with various functional groups (i.e. films with a variety of surface energies) as heterogeneous nucleation sites to investigate polymorph control in a model organic chemical compound.

## 1.4 References

1. Lee, A. Y.; Erdemir, D.; Myerson, A. S., Crystal Polymorphism in Chemical Process Development. *Annual Review of Chemical and Biomolecular Engineering*, **2011**, 2, 259-280
2. Diao, Y. et al. Understanding Polymorphism in Organic Semiconductor Thin Films through Nanoconfinement, *J. Am. Chem. Soc.*, **2014**, 136, 17046–17057
3. Yu, L., Polymorphism in Molecular Solids: An Extraordinary System of Red, Orange, and Yellow Crystals. *Acc. Chem. Res.*, **2010**, 43, 1257–1266
4. Yu, L., Color Changes Caused by Conformational Polymorphism: Optical-Crystallography, Single-Crystal Spectroscopy, and Computational Chemistry. *J. Phys. Chem. A*, **2002**, 106, 544–550
5. Pudipeddi, M.; Serajuddin, A. T. M., Trends in solubility of polymorphs. *J. Pharm. Sci.* **2005**, 94, 929–939
6. Polte, J., Fundamental growth principles of colloidal metal nanoparticles – a new perspective, *CrystEngComm*, **2015**, 17, 6809-6830
7. Kitamura, M., Strategy for control of crystallization of polymorphs. *CrystEngComm*, **2009**, 11, 949-964
8. Morissette, S. L.; Almarsson, O.; Peterson, M. L.; Remenar, J. F.; Read, M. J.; Lemmo, A. V.; Ellis, S.; Cima, M. J.; Gardner, C. R., High-throughput crystallization: polymorphs, salts, co-crystals and solvates of pharmaceutical

- solids. *Adv. Drug Deliv. Rev.* **2004**, *56*, 275-300.
9. Detoisien, T.; Forite, M.; Taulelle, P.; Teston, J.; Colson, D.; Klein, J. P.; Veessler, S., A rapid method for screening crystallization conditions and phases of an active pharmaceutical ingredient, *Organic Process Research & Development*, **2009**, *13*, 1338-1342.
  10. Jiang, Q.; Ward, M. D., Crystallization under nanoscale confinement. *Chem. Soc. Rev.*, **2014**, *43*, 2066-2079
  11. Diao, Y.; Harada, T.; Myerson, A. S.; Hatton, T. A.; Trout, B. L., The role of nanopore shape in surface-induced crystallization, *Nature Materials* **2011**, *10*, 867–871
  12. Diao, Y.; Whaley, K. E.; Helgeson, M. E.; Woldeyes, M. A.; Doyle, P. S.; Myerson, A. S.; Hatton, T. A.; Trout, B. L. Gel-Induced Selective Crystallization of Polymorphs, *J. Am. Chem. Soc.*, **2012**, *134*, 673–684
  13. Torbeev, V. Y.; Shavit, E.; Weissbuch, I.; Leiserowitz, L.; Lahav, M. Control of Crystal Polymorphism by Tuning the Structure of Auxiliary Molecules as Nucleation Inhibitors. The  $\beta$ -Polymorph of Glycine Grown in Aqueous Solutions, *Cryst. Growth Des.* **2005**, *5*, 2190–2196
  14. Mitchell, C. A.; Yu, L.; Ward, M. D., Selective Nucleation and Discovery of Organic Polymorphs through Epitaxy with Single Crystal Substrates, *J. Am. Chem. Soc.* **2001**, *123*, 10830-10839.
  15. Carter, P. W.; Ward, M. D., Directing Polymorph Selectivity During Nucleation of Anthranilic Acid on Molecular Substrates, *J. Am. Chem. Soc.* **1994**, *116*, 769-770.
  16. Carter, P. W.; Ward, M. D., Topographically directed nucleation of organic

- crystals on molecular single-crystal substrates, *J. Am. Chem. Soc.* **1993**, 115, 11521-11535.
17. Bonafede, S. J.; Ward, M. D., Selective Nucleation and Growth of an Organic Polymorph by Ledge-Directed Epitaxy on a Molecular Crystal Substrate, *J. Am. Chem. Soc.* **1995**, 117, 7853-7861.
  18. Price, P. C., Grzesiak, A. L., Matzger, A. J., Crystalline Polymorph Selection and Discovery with Polymer Heteronuclei, *J. Am. Chem. Soc.* **2005**, 127, 5512-5517
  19. Zhang, J.; Liu, A.; Han, Y.; Ren, Y.; Gong, J.; Li, W.; Wang, J., Effects of Self-Assembled Monolayers on Selective Crystallization of Tolbutamide, *Cryst. Growth Des.* **2011**, 11, 5498-5506
  20. Aizenberg, J.; Black, A. J.; Whitesides, G. M., Control of crystal nucleation by patterned self-assembled monolayers, *Nature* **1999**, 398, 495-498
  21. Love, J. C.; Estroff, L. A.; Kriebel, J. K.; Nuzzo, R. G.; Whitesides, G. M., Self-Assembled Monolayers of Thiolates on Metals as a Form of Nanotechnology, *Chem. Rev.*, **2005**, 105, 1103–1170
  22. Singh, A.; Lee, I. S.; Kim, K.; Myerson, A. S., Crystal growth on self-assembled monolayers, *CrystEngComm*, **2011**, 13, 24-32
  23. Porter, M. D.; Bright, T. B.; Allara, D. L.; Chidsey, C. E. D. J., Spontaneously organized molecular assemblies. 4. Structural characterization of n-alkyl thiol monolayers on gold by optical ellipsometry, infrared spectroscopy, and electrochemistry, *Am. Chem. Soc.* **1987**, 109, 3559-3568.
  24. Mani, G.; Johnson, D. M.; Marton, D.; Dougherty, V. L.; Feldman, M. D.; Patel,

- D.; Ayon, A. A.; Agrawal, C. M., Stability of self-assembled monolayers on titanium and gold, *Langmuir*, **2008**, 24, 6774–6784
25. Wang, M.; Liechti, K.M.; Wang, Q.; White, J. M., Self-assembled silane monolayers: Fabrication with nanoscale uniformity, *Langmuir*, **2005**, 21, 1848–1857
26. Wang, Y.; Lieberman, M. Growth of Ultrasooth Octadecyltrichlorosilane Self-Assembled Monolayers on SiO<sub>2</sub>, *Langmuir*, **2003**, 19, 1159–1167
27. Silberzan, L. L.; Ausserre, D.; Benattar, J. J. Silanation of silica surfaces. A new method of constructing pure or mixed monolayers, *Langmuir*, **1991**, 7, 1647–1651
28. Helmy, R.; Fadeev, A. T., Self-Assembled Monolayers Supported on TiO<sub>2</sub>: Comparison of C<sub>18</sub>H<sub>37</sub>SiX<sub>3</sub> (X = H, Cl, OCH<sub>3</sub>), C<sub>18</sub>H<sub>37</sub>Si(CH<sub>3</sub>)<sub>2</sub>Cl, and C<sub>18</sub>H<sub>37</sub>PO(OH)<sub>2</sub>, *Langmuir*, **2002**, 18, 8924–8928

## **Chapter 2. Self-assembled monolayers (SAMs) as Nucleating Surfaces to Study Crystallographic Polymorphs**

### **2.1 INTRODUCTION**

Polymorphism is a phenomenon in which a compound crystallizes into more than one solid state crystal structure. Polymorphs of the same compound have different properties, such as melting point, solid density, mechanical hardness, dissolution rate, and bioavailability, which are important parameters in drug use.<sup>1</sup> Therefore, the understanding and control of polymorphism is noteworthy in many industrial applications, especially for pharmaceuticals. For these reasons, it is beneficial to develop methods for studying the role of solvent and substrate chemistries on polymorph selection.

Traditionally, polymorphs are identified through time-consuming methodologies such as exhaustive screens of different solvents, cooling or evaporation rates, and supersaturation levels to discover as many polymorphs as possible.<sup>1-3</sup> Current methods for discovery and control of polymorphs include nano-confinement<sup>4-6</sup>, small molecular additives<sup>7,8</sup>, polymer heteronuclei<sup>9</sup>, and epitaxial nucleation on single crystal substrates.<sup>10-13</sup> Recently, several researchers have used self-assembled monolayers (SAMs) as the nucleation substrate to alter the energetic barrier to the nucleation of different polymorphs. For example, Jingkang Wang and his co-workers achieved selective crystallization of tolbutamide on SAMs with methyl, trifluoromethyl, and phenyl functional groups.<sup>14</sup> The Aizenberg group demonstrated that well-defined patterned SAMs can induce nucleation of calcite polymorphs with specific

orientations.<sup>15</sup> Myerson has a review paper on the crystal polymorphism in chemical process development.<sup>16</sup> In this review paper, it is discussed that polymorphism control can be obtained by the design of SAMs with various surface chemistries, which introduce ionic or hydrogen-bonding interactions among SAMs and solute molecules. Despite this progress, however, comprehensive understanding of the parameters that control polymorph selection on SAMs remains a challenge.

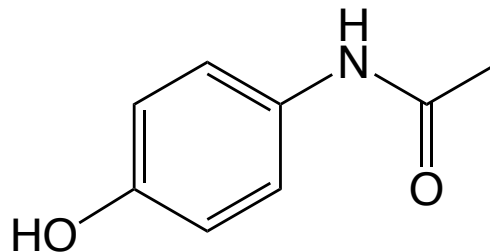


**Figure 1.** Acetaminophen(ACM)

Acetaminophen (ACM) is a well studied active pharmaceutical ingredient (API) for reducing pain and fever.<sup>17</sup> ACM has two well-known polymorphs, a monoclinic form I and an orthorhombic form II. Metastable form II is more soluble in aqueous environments and more compressible for tableting because of a layer-by-layer type packing of ACM molecules in the associated crystal structure.<sup>18</sup> The favorable properties of form II allured scientists to find a route to crystallize ACM polymorphs selectively and efficiently. For example, the Wilson Group has selectively produced form II by recrystallizing ACM from solutions composed of monosubstituted halobenzoic acid, which they called a multicomponent crystallization technique.<sup>19</sup> Matzger and his coworkers also achieved ACM polymorph selection by use of heterogeneous nucleation on polymer surfaces in aqueous solutions.<sup>9, 20</sup>

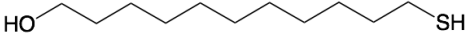
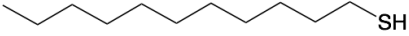
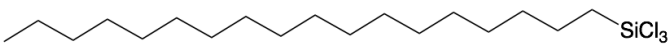
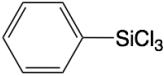
In the present work we examined 1-undecanethiol (UDT) and 11-mercapto-1-undecanol (MUOH) SAM chemistries on gold, and trichloro(octadecyl)silane (OTS)

and trichloro(phenyl)silane (PTS) on oxide bearing silicon substrates in the presence of various solvent systems to investigate their ability to influence the nucleation, polymorph selection and crystal growth of acetaminophen (ACM). Our work may help the community to identify rational design criteria for the choice of SAMs and associated solvents to study polymorph selection and crystal orientation for small organic molecule crystallization.

## **2.2 EXPERIMENTAL SECTION**

**2.2.1 Materials.** 11-mercapto-1-undecanol (99%, Sigma-Aldrich), 1-undecanethiol (98%, Sigma-Aldrich), trichloro(phenyl)silane ( $\geq 97\%$ , Sigma-Aldrich), trichloro(octadecyl)silane ( $\geq 90\%$ , Sigma-Aldrich), anhydrous hexane (95%, Sigma-Aldrich), anhydrous 1,4-dioxane (99.8%, Sigma-Aldrich), molecular sieves 4Å (Sigma-Aldrich), gold-coated silicon wafers (Platypus Technologies), silicon wafers (WRS Materials), acetaminophen (98%, Sigma-Aldrich), ethanol (200 Proof, KOPTEC), and acetone (MACRON) were used as received. The structure of various chemicals used in this study for SAM formation is shown in Table 1.

**Table 1.** Chemical structures of molecules used for SAM formation

<i>SAMs molecule</i>	<i>Chemical structure</i>
11-mercapto-1-undecanol (MUOH)	
1-undecanethiol (UDT)	
Trichloro(octadecyl)silane (OTS)	
Trichloro(phenyl)silane (PTS)	

### 2.2.2 Gold substrate preparation and surface modification by thiol-gold chemistry.

Gold coated silicon wafers were cut into 2 cm by 1 cm substrates and then sonicated in deionized (DI) water, followed by washing in ethanol for 2 mins each. Each gold coated silicon wafer was plasma cleaned for 5 mins at “high” level to remove organic impurities on the surface. The plasma-cleaned wafer was then moved into a vial. The vial was sealed with parafilm and purged in dry N<sub>2</sub> for 15 seconds to create N<sub>2</sub> atmosphere inside the vial. Thiol solutions (10 mM) in ethanol were prepared and sonicated for 5 mins to be homogenized before use. Homogenized 5 mL thiol solution was injected into the vial. After 24 hours at room temperature, wafers were sonicated in fresh ethanol for 2 mins and blow-dried with N<sub>2</sub>.<sup>21, 22</sup>

**2.2.3 Silica substrate preparation and surface modification by silane-silica chemistry.** Silicon wafers were cut into 2 cm by 1 cm size and then sonicated in acetone

for 5 mins. Each silicon wafer was plasma cleaned for 5 mins at high level to remove organic impurities from the surface. The plasma-cleaned wafer was moved into a vial. The vial was sealed with parafilm and purged with dry N<sub>2</sub> for 15 seconds to create N<sub>2</sub> atmosphere inside the vial. Silane solution (10 mM) was made by mixing silane and hexane in a glove box, in which the O<sub>2</sub> concentration was below 10 ppm and H<sub>2</sub>O concentration was below 1 ppm. 5 mL silane-in-hexane solution was injected into the vial. After 24 hours at room temperature, wafers were sonicated in fresh acetone for 5 mins and blow-dried with N<sub>2</sub>.<sup>23</sup>

**2.2.4 Solution preparation.** To prepare the ACM/water solution, 30 mg of ACM was first added to 2 mL of DI water and heated to 45 °C until complete dissolution.<sup>20</sup> The solution was then cooled to room temperature.

The polar solvents, ethanol and 1,4-dioxane, were dried over 4Å molecular sieves and filtered via 0.2 µm PTFE syringe filter right before the solvent was used to dissolve ACM. Drying of solvents and subsequent filtering were steps found to be key to obtaining reproducible results for all studies.

To prepare the ACM/ethanol solution, 30 mg of ACM was first added to 2 mL of anhydrous ethanol, which was dried by molecular sieves and subsequently filtered by 0.2 micron PTFE syringe filter. The solution was heated to 45 °C and cooled to room temperature before use.<sup>24</sup>

To prepare the ACM/1,4-dioxane solution, 30 mg of ACM was first added to 2 mL of anhydrous 1,4-dioxane, which was dried by molecular sieves and subsequently filtered

by 0.2 micron PTFE syringe filter. The solution was heated up 45 °C and cooled to room temperature before use.

To prepare the ACM solution with water and 1,4-dioxane, 30 mg of ACM was first added to a 2 mL mixture of water and anhydrous 1,4-dioxane with a 20 to 80 volume ratio. 1,4-dioxane was dried by molecular sieves and then filtered by 0.2 micron PTFE syringe filter. Water was also filtered by 0.2 micron PTFE syringe filter before use. The ACM solution was heated up 45 °C and cooled to room temperature before use.

**2.2.5 Crystallization.** A crystal growth chamber (Figure 2) was designed to conduct the crystallization experiments on the various SAMs. Using a micropipette, approximately 10  $\mu$ L droplets of the various ACM solutions (15 mg/mL) were placed onto the SAM-functionalized surface. A dome was used to protect samples from contamination (e.g., dust in air). The space between dome and substrate allowed air flow, so that droplet evaporation occurred under atmospheric pressure under the dome inducing crystallization. Using this crystallization set-up (Fig. 2), one substrate can hold multiple droplets to crystallize simultaneously. The number of droplets per substrate depended on size and wettability of the substrate, and solvent type of the ACM solution. On hydrophobic surfaces (UDT, OTS, PTS), each substrate (1 cm\*2 cm) generally held 3 droplets for crystallization, while on hydrophilic surfaces (MUOH), a single droplet (10  $\mu$ L) could spread and eventually almost fully cover the substrate.

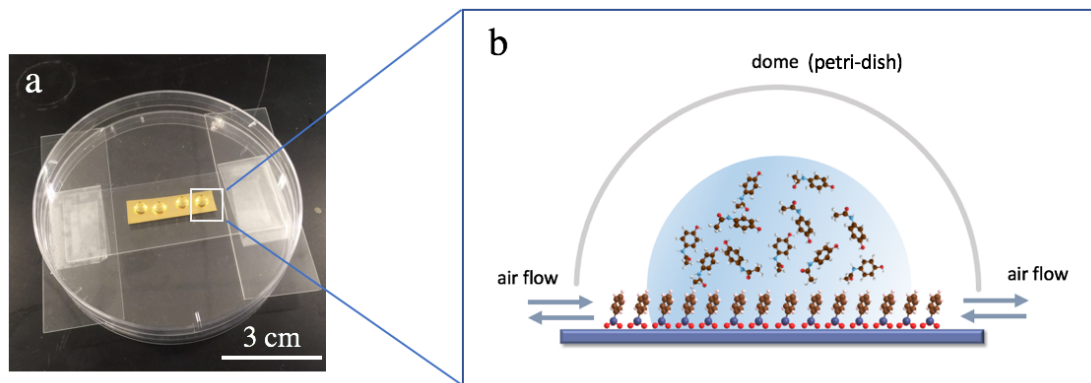


**Figure 2.** Crystallization set-up for droplet experiments: a) 4 droplets of ACM solution on an UDT-covered gold coated wafer at room temperature. b) Schematic of droplet experiments on SAM-modified substrates viewed from the side.

### 2.2.6 Characterization of ACM crystals

The polymorph derived from the droplet evaporation experiments was determined by using a Bruker D8 General Area Detector Diffraction System (GADDS) with CuK $\alpha$  radiation and operating at 40 kV and 40 mA. To ensure measuring one sample on the substrate at a time, the slit size was selected at 0.5 mm and the desired sample volume was selected and centered by using a camera attached to the instrument. Additionally, Ni 0.02 was selected as the beam filter to maximize signal to noise. The instrumental set up was set to “Coupled TwoTheta/Theta” scan type and “Step” scan mode. DIFFRAC.EVA software by Bruker was used to analyze the raw XRD data and 2D X-ray patterns were integrated azimuthally to obtain 1D scans.

In addition to x-ray diffraction, samples were characterized by scanning electron microscopy (SEM) on a Tescan-Mira3-SEM by sputter-coating sample surfaces with gold and platinum on a DESK V sputter coater from DENTON VACUUM Company. SEM images were collected by in-beam SE detector and the beam energy was 5 kV.

## 2.3 RESULTS

### 2.3.1 Growth of ACM on Hydrophobic SAMs (UDT, OTS, PTS): Role of Solvent on Polymorph Selectivity.

Three different hydrophobic SAMs, UDT, OTS, and PTS, were used as substrates for the crystallization of ACM. Droplets of ACM solution (15 mg/mL) were placed on the SAMs and allowed to evaporate, ensuring that nucleation occurred on the substrate (Fig. 2). Three polar solvents were initially tested: water, ethanol, and 1,4-dioxane. After complete evaporation of the solvent, the polymorph formed in each droplet was determined by powder x-ray diffraction (Fig. 3).

Importantly, each droplet was converted into a pure crystal polymorph: either orthorhombic (form I) or monoclinic (form II). For all combinations between the 3 hydrophobic SAMs and 3 polar solvents, form I, the thermodynamically most stable polymorph, formed in the majority of droplets (Table 2). In contrast, when a 20:80 water:dioxane mixture was used as the solvent, the polymorph selectivity on all three SAMs switched to form II becoming the dominant polymorph (Table 2).

Interestingly, droplet experiments with water/dioxane mixtures on UDT, OTS, and PTS, formed a stable glass-like state, which generally took two days to fully crystallize (relative to generally less than 12 hours for all other experiments).

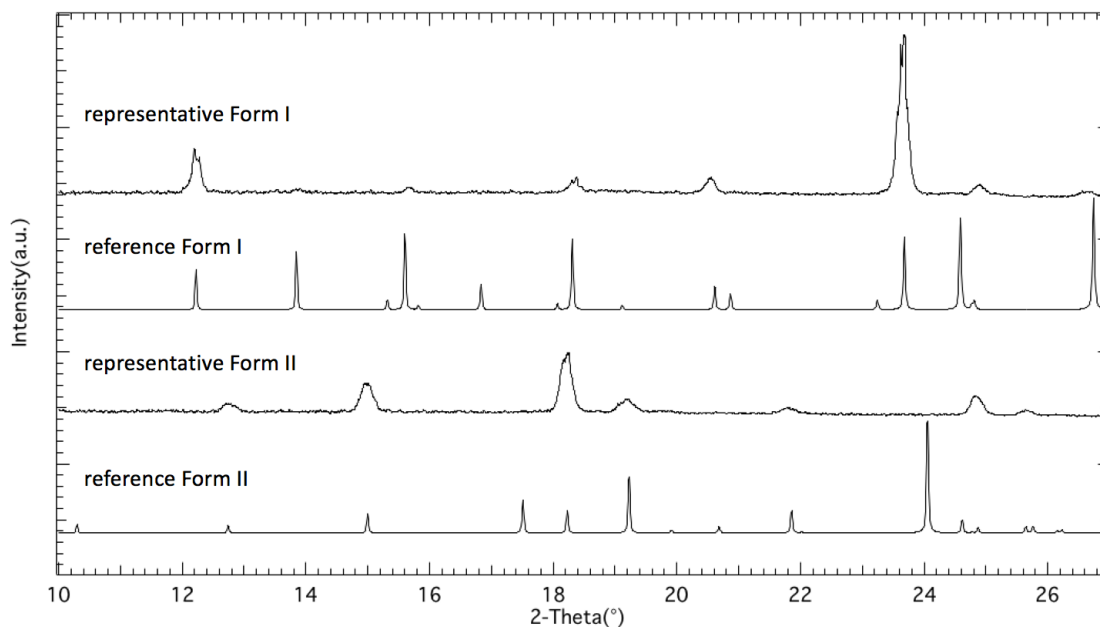


**Figure 3.** Representative XRD data for crystallization of ACM Form I (UDT/water) and Form II (PTS/ water & dioxane), and XRD data of reference Form I and Form II is simulated using VESTA (Visualization of Electronic and Structural Analysis).<sup>25,26</sup>

**Table 2.** Crystallization results for combinations of different SAM chemistries with various solvents.  $n$  = number of droplets in the study.

<i>Solvent</i>	<i>SAM Chemistry</i>	<i>n</i>	<i>Form I</i>	<i>Form II</i>
Ethanol	UDT	20	<b>80%</b>	20%
	OTS	18	<b>94%</b>	6%
	PTS	14	<b>93%</b>	7%
	MUOH	11	9%	<b>91%</b>
Water	UDT	9	<b>93%</b>	7%
	OTS	15	<b>87%</b>	13%
	PTS	10	<b>100%</b>	0%
	MUOH	17	<b>100%</b>	0%
1,4-dioxane	UDT	11	<b>100%</b>	0
	OTS	10	<b>90%</b>	10%
	PTS	10	<b>70%</b>	30%
	MUOH	10	20%	<b>80%</b>
Water/dioxane 20/80	UDT	11	9%	<b>91%</b>
	OTS	11	0	<b>100%</b>
	PTS	9	0	<b>100%</b>
	MUOH	10	0	<b>100%</b>

### **2.3.2 Growth of ACM on a Hydrophilic SAM (MUOH): Role of Solvent and**

**Substrate on Polymorph Selectivity.** As a comparison to the hydrophobic SAMs, droplet experiments were performed on a hydrophilic SAM on gold formed by MUOH (Table 2), which has the same chain length as UDT. Using water as solvent, 100% of the droplets crystallized on MUOH SAMs generated form I. Moreover, for crystallization from the 20:80 water/dioxane mixture, MUOH SAMs induced nucleation of Form II. Both of these results were similar to those of the hydrophobic SAMs. In contrast to the hydrophobic SAMs, however, with either dioxane or ethanol as solvents, form II rather than form I preferentially formed on the hydrophilic MUOH SAMs (Table 2). These results suggest that solvent and substrate work together to dictate which polymorph of ACM forms.

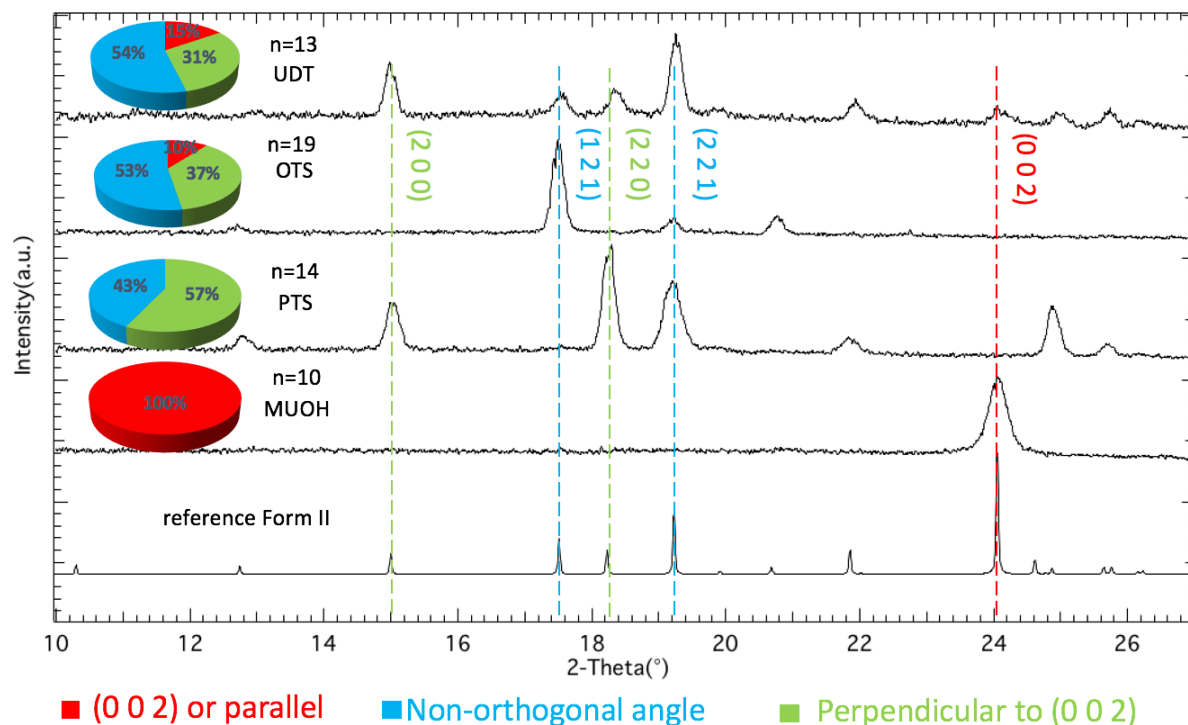


**Figure 4.** XRD data for crystallization of ACM on UDT, OTS, PTS, and MUOH

SAM chemistries with a mixture of water and dioxane used as solvent. Red indicates diffraction peaks from the crystal plane (0 0 2) and parallel ones. Blue indicates peaks from crystal planes not orthogonal to the plane (0 0 2). Green indicates peaks of crystal planes perpendicular to the plane (0 0 2), such as (2 0 0). XRD data of reference form II is simulated using VESTA (Visualization of Electronic and Structural Analysis).<sup>26</sup> Each pie chart summarizes the major x-ray diffraction peaks contributing to a diffractogram for a specific SAM surface chemistry.

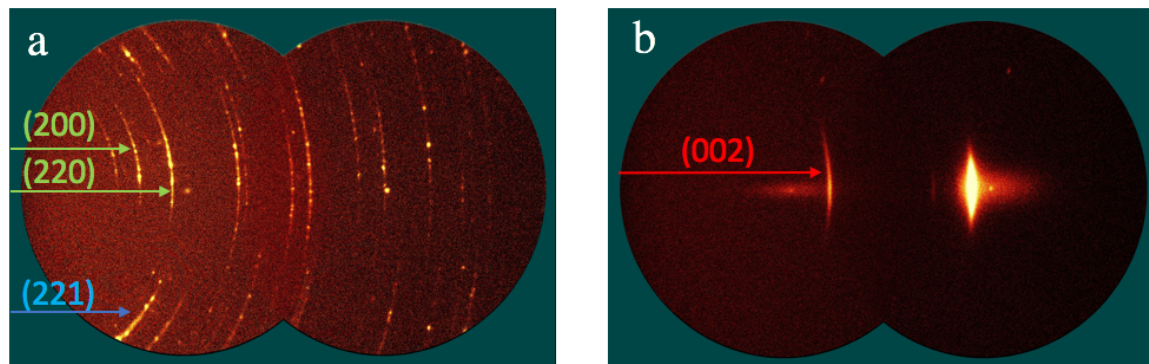


**Figure 5.** 2D X-ray Diffraction patterns for ACM crystallized on PTS (a) and MUOH (b) based surfaces with a water/dioxane (20:80 v/v) mixture as solvent. Red indicates peaks of crystal plane (0 0 2) and parallel ones. Blue indicates peaks of crystal planes not orthogonal to plane (0 0 2). Green indicates peaks of crystal planes perpendicular to the plane (0 0 2), such as (2 0 0).

### 2.3.3 Different crystal orientations from different SAM surface chemistries.

Having identified solvent/substrate pairs that strongly favored the growth of the polymorph form II of ACM, we used x-ray diffraction to further probe effects of the surface chemistry on specifics of the crystallization. Specifically, we compared the  $\theta - 2\theta$  diffraction patterns of Form II crystals grown on all four different SAMs from a 20:80 water:dioxane mixture (Fig. 5). In this scattering geometry, planes parallel to the substrate scatter more strongly and therefore peak intensities can be used to evaluate crystal orientation. For crystals grown on hydrophobic SAMs, e.g., UDT, OTS, and PTS, the majority (>80%) of the reflections are from planes perpendicular to the (002) plane, e.g.,  $\{hk0\}$  planes, and other non-orthogonal planes, e.g.,  $\{hk1\}$  planes. For PTS, this texturing is pronounced with no occurrence of  $\{00l\}$  reflections.

In contrast, on the hydrophilic MUOH substrate, reflections from  $\{00l\}$  planes accounts for 100% of all reflections, which indicates highly oriented crystals. Since PTS and MUOH substrates appear to impart the strongest crystallographic texture to Form II crystals, we examined 2-D diffraction patterns for these materials (Fig. 5). For as-grown crystals on PTS modified substrate, powder-like arcs are observed for most reflections, with the notable exception of the  $(0\ 0\ 2)$  reflection. The powder-like arcs indicate some tilt of the  $\{hk0\}$  planes normal to the substrate. For as-grown crystals on MUOH modified substrate, only the  $(0\ 0\ 2)$  reflection is observed, with a narrow azimuthal spread, indicating minimal tilt of the  $(002)$  normal to the substrate.

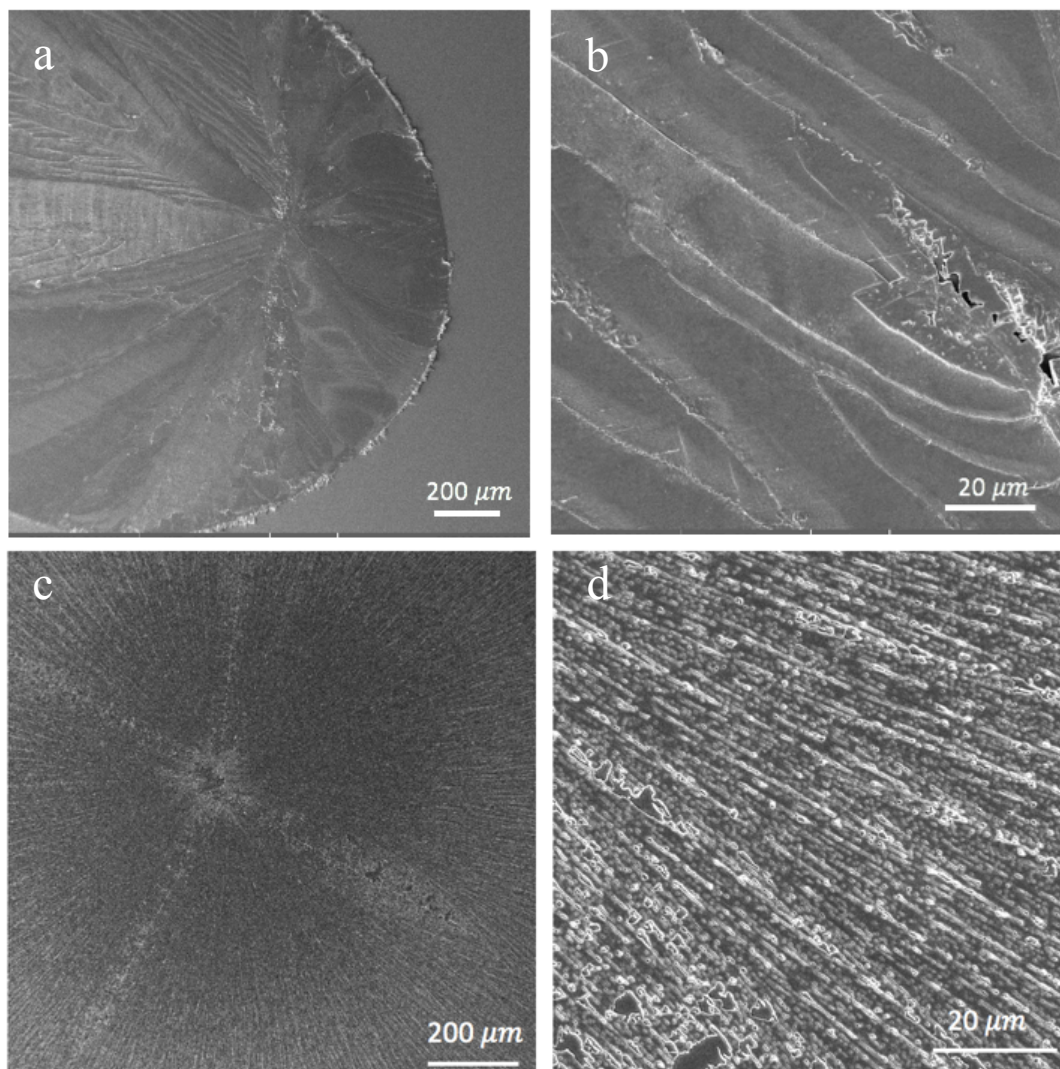


**Figure 6.** SEM images at two different magnifications of Form II surface morphology on PTS (a,b) and MUOH (c, d) SAMs grown from 20:80 water:dioxane.

**2.3.4 Surface morphology of ACM crystals on PTS and MUOH.** SEM images, shown in Fig. 6, reveal morphology and surface texture of the Form II crystals when grown on PTS and MUOH SAMs, respectively. On both substrates, spherulitic-like growth is observed with radiating crystallites from a central location. On PTS modified surfaces (Fig. 6 a,b), however, the crystals appear larger and flatter than

those on MUOH (Fig. 6 c,d). This difference in morphology is most likely related to the different crystallographic textures observed by x-ray diffraction and the preferred growth habits along different directions.

## 2.4 DISCUSSION

### **Growth of ACM on Hydrophobic SAMs (UDT, OTS, PTS): Role of Solvent on**

**Polymorph Selectivity** Three different hydrophobic SAMs, UDT, OTS, and PTS, were initially used as substrates for the crystallization of ACM from three polar solvents, water, ethanol, and 1,4-dioxane. By XRD characterization, the majority of samples crystallized as Form I, the thermodynamically stable polymorph. The surface free energy of UDT SAMs should be similar to that of OTS, since both UDT and OTS SAMs share the methyl terminated surface chemistry. However, differences in the number of methylene ( $-\text{CH}_2-$ ) units in the SAM backbone causes changes in surface free energy. According to previous studies, the surface free energy of SAMs with an odd number of methylene units in the backbone, is systematically larger than that of SAMs with an even number of methylene units.<sup>27-30</sup> Obviously, the surface free energy of PTS SAMs is not the same as that of UDT and OTS, because of the distinctive phenyl functional group on PTS. Nonetheless, after introducing three solvents, water, ethanol, and 1,4-dioxane, the variation of surface energy among three SAMs does not lead to any changes of polymorph preference. In comparison, with 20:80 water:dioxane used as solvent, Form II on these three hydrophobic SAMs became

dominant among results. Therefore, according to classical nucleation theory, the water/dioxane mixture solvent plays a decisive role in polymorph selectivity by changing solvent-crystal and solvent-substrate interfacial energies.

In conclusion, these results show that polymorph selection is not strongly sensitive to the specific hydrophobic surface chemistry: UTO, OTS, or PTS. However, with respect to solvent effects, we find that ACM crystallization in a mixture of water and 1,4-dioxane results in form II, on all three hydrophobic SAMs, while either pure water or pure 1,4-dioxane primarily yields Form I. While we don't fully understand the mechanism that yields form II over form I in the mixed solvent system, the appearance of a "glassy-state" type droplet on all three hydrophobic SAMs when grown from water:dioxane may play a role in the polymorph selectivity observed in these systems.

**Comparison of ACM polymorph control between hydrophobic (UDT) and hydrophilic (MUOH) SAM chemistries with various solvents.** As a comparison to hydrophobic (*e.g.* UDT) surface chemistry, droplet experiments were performed on hydrophilic (MUOH) SAMs. With respect to hydrophilic SAM selection, we chose MUOH to do droplet experiments as its alkyl spacer chain length is exactly the same as for UDT. With water and water/dioxane mixtures, crystallization results on MUOH were similar to that on UDT. In contrast, with dioxane as solvent while 100% of the results on UDT were form I, the majority (80%) of crystallization results on MUOH showed form II. Similar results to dioxane were observed for crystallization on UDT

versus MUOH surfaces from ethanol, see Table 2. These results again point to the fact that surface chemistry and solvent effects play a role. The Matzger group has used polymers as substrates for heterogeneous crystallization of ACM from aqueous solutions.<sup>9, 20</sup> In their work, metastable orthorhombic form II is induced on the hydrophobic polyethylene (PE) substrate, which is different from our results on UDT or MUOH SAMs both preferentially showing form I. However, in their study when moving from PE to poly(methyl methacrylate) (PMMA) polymorph selection switches from form II to form I. This comparison suggests that even with similar surface chemistry, heteronucleation guided polymorph control is different between polymers and SAMs. This can probably be attributed to the variance in surface ordering. In our case, for water containing systems, polymorph selection is independent of substrate chemistry, whether hydrophobic or hydrophilic. However, for pure organic solvents like ethanol or dioxane, the polymorph switches from form I to form II when SAM surface chemistry is changed from hydrophobic to hydrophilic.

#### **Different SAM surface chemistry results in different crystal orientation.**

Using a 20:80 water/dioxane mixture as the crystallization solvent, Form II crystallized on both PTS and MUOH surfaces, but the observed orientation of the crystal is vastly different depending on surface chemistry. From analysis of the 2-D x-ray diffraction patterns, we can propose a model of the molecular interaction between Form II of ACM and PTS and MUOH SAMs (Fig. 7). The phenyl ring of ACM is oriented parallel to the (002) plane in Form II. From our results, we see a strong

influence of the substrate chemistry on dictating the relative orientation of the ACM phenyl ring with the substrate. The PTS substrate is composed of phenyl rings slightly tilted away from normal to the substrate.<sup>31, 32</sup> The x-ray diffraction results show that on the PTS substrate, the ACM molecules align such that the phenyl rings are approximately perpendicular to the substrate (Fig. 7a). The powder-like arcs in the 2-D pattern are indicative of some rotational variation around the (200) and similar planes, which will still keep the phenyl rings perpendicular to the substrate. The (002) reflection is never observed for crystals grown on PTS substrates, i.e., the cleavage planes in which the phenyl rings lie (red) are always perpendicular to the substrate.

In contrast, on the MUOH SAM, the Form II crystals grow such that the phenyl rings are approximately parallel to the substrate (Fig. 7b). Some azimuthal spread of the (002) reflection indicates that there is some tilt in the orientation – not all cleavage planes are perfectly parallel to the substrate. The absence of all other reflections suggests that there is a strong preference for the phenyl rings of ACM to lie parallel to the hydrophilic substrate.

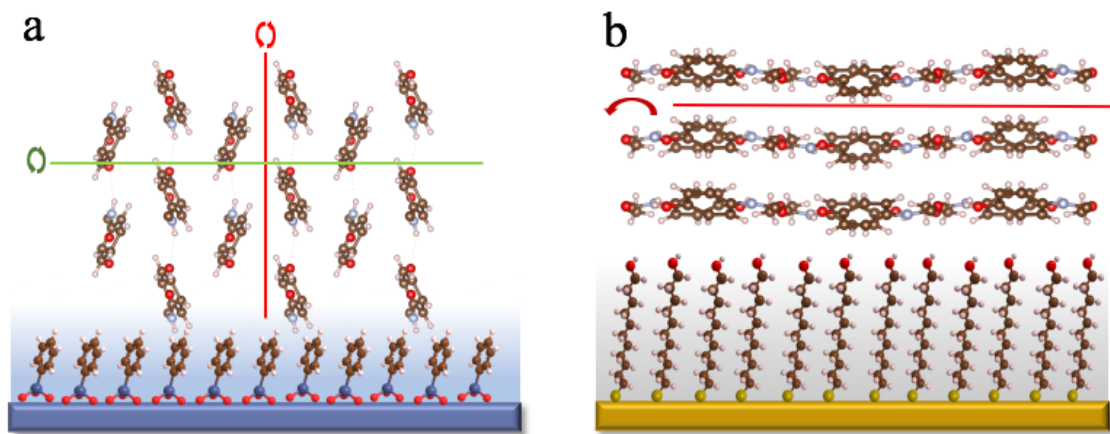


**Figure 7.** Schematic representation of the proposed molecular interaction between Form II crystals and different SAMs. Form II crystallized (a) on PTS SAMs with (200) orientation and (b) on MUOH SAMs with (002) orientation. Red lines indicate crystal planes parallel to (0 0 1). The green line indicates crystal planes perpendicular to the (0 0 2) plane, such as the (2 0 0) plane. Arrows indicate angular variations around the assigned directions leading to the observed diffraction patterns.

## 2.5 CONCLUSION

We examined 1-undecanethiol (UDT) and 11-mercapto-1-undecanol (MUOH) SAM chemistries on gold, as well as trichloro(octadecyl)silane (OTS), and trichloro(phenyl)silane (PTS) on silicon in the presence of various solvent systems to investigate their ability to influence the nucleation, crystal growth, and polymorph selection of a common drug, acetaminophen (ACM). On hydrophobic surfaces, use of pure solvents resulted in ACM form I, while a mixture of water and dioxane produced form II. In general, both solvent and SAM surface chemistry act in concert to control

polymorph selection. In addition to polymorph selection, we observed that for form II different SAM surface chemistries influence crystal orientation. The phenyl-terminated SAM surface nucleated crystals with the phenyl rings oriented approximately perpendicularly to the substrate (e.g. (200), (211) and (210) planes lie parallel to the substrate). In contrast,  $-OH$  group terminated SAM surfaces promoted crystallization with the (002) cleavage plane oriented parallel to the substrate. This work provides a new paradigm for acetaminophen polymorph control, where solvent and substrate chemistry work in concert to control polymorphism. Furthermore, we expect that our method will contribute to understanding the role of solvent and substrate in heterogeneous nucleation and, also, the process of polymorph crystallization.

## **ACKNOWLEDGMENTS**

This research was supported by the International Fine Particle Research Institute and by the Cornell Center for Materials Research with funding from the NSF MRSEC program (DMR-1120296). The authors are grateful to Dr. Kate Barteau for the thoughtful discussion about the results in this paper.

## 2.6 REFERENCES

1. Lee, A. Y.; Erdemir, D.; Myerson, A. S., Crystal Polymorphism in Chemical Process Development, *Annual Review of Chemical and Biomolecular Engineering*, **2011**, 2, 259-280
2. Morissette, S. L.; Almarsson, O.; Peterson, M. L.; Remenar, J. F.; Read, M. J.; Lemmo, A. V.; Ellis, S.; Cima, M. J.; Gardner, C. R., High-throughput crystallization: polymorphs, salts, co-crystals and solvates of pharmaceutical solids, *Adv. Drug Deliv. Rev.* **2004**, 56, 275-300.
3. Detoisien, T.; Forite, M.; Taulelle, P.; Teston, J.; Colson, D.; Klein, J. P.; Veessler, S., A rapid method for screening crystallization conditions and phases of an active pharmaceutical ingredient, *Organic Process Research & Development*, **2009**, 13, 1338.
4. Jiang, Q.; Ward, Crystallization under nanoscale confinement, M. D., *Chem. Soc. Rev.*, **2014**, 43, 2066-2079
5. Diao, Y.; Harada, T.; Myerson, A. S.; Hatton, T. A.; Trout, B. L., The role of nanopore shape in surface-induced crystallization, *Nature Materials* **2011**, 10, 867–871
6. Diao, Y.; Whaley, K. E.; Helgeson, M. E.; Woldeyes, M. A.; Doyle, P. S.; Myerson, A. S.; Hatton, T. A.; Trout, B. L., Gel-Induced Selective Crystallization of Polymorphs, *J. Am. Chem. Soc.*, **2012**, 134, 673–684
7. Kitamura, M., Strategy for control of crystallization of polymorphs, *CrystEngComm*, **2009**, 11, 949-964

8. Torbeev, V. Y.; Shavit, E.; Weissbuch, I.; Leiserowitz, L.; Lahav, M., Control of Crystal Polymorphism by Tuning the Structure of Auxiliary Molecules as Nucleation Inhibitors. The  $\beta$ -Polymorph of Glycine Grown in Aqueous Solutions, *Cryst. Growth Des.* **2005**, 5, 2190–2196
9. Price, P. C.; Grzesiak, A. L.; Matzger, A. J., Crystalline Polymorph Selection and Discovery with Polymer Heteronuclei, *J. Am. Chem. Soc.* **2005**, 127, 5512-5517
10. Mitchell, C. A.; Yu, L.; Ward, M. D., Selective nucleation and discovery of organic polymorphs through epitaxy with single crystal substrates, *J. Am. Chem. Soc.* **2001**, 123, 10830-10839.
11. Carter, P. W.; Ward, M. D., Directing Polymorph Selectivity During Nucleation of Anthranilic Acid on Molecular Substrates, *J. Am. Chem. Soc.* **1994**, 116, 769-770.
12. Carter, P. W.; Ward, M. D., Topographically directed nucleation of organic crystals on molecular single-crystal substrates, *J. Am. Chem. Soc.* **1993**, 115, 11521.
13. Bonafede, S. J.; Ward, M. D., Selective Nucleation and Growth of an Organic Polymorph by Ledge-Directed Epitaxy on a Molecular Crystal Substrate, *J. Am. Chem. Soc.* **1995**, 117, 7853-7861.
14. Zhang, J.; Liu, A.; Han, Y.; Ren, Y.; Gong, J.; Li, W.; Wang, L., Effects of Self-Assembled Monolayers on Selective Crystallization of Tolbutamide, *Cryst. Growth Des.* **2011**, 11, 5498-5506
15. Aizenberg, J.; Black, A. J.; Whitesides, G. M., Control of crystal nucleation by patterned self-assembled monolayers, *Nature* **1999**, 398, 495-498
16. Singh, A.; Lee, I. S.; Kim, K.; Myerson, A. S., Crystal growth on self-assembled

- monolayers, *CrystEngComm*, **2011**, 13, 24-32
17. Stojaković, J.; Baftizadeh, F.; Bellucci, M. A.; Myerson, S. A.; Trout, B. L., Angle-Directed Nucleation of Paracetamol on Biocompatible Nanoimprinted Polymers, *Cryst. Growth Des.*, **2017**, 17, 2955–2963
  18. Fachaux, J. M.; Guyot-Hermann, A. M.; Guyot, J. C.; Conflant, P.; Darche, M.; Veessler, S.; Boistelle, R., Pure paracetamol for direct compression, *Powder Technology*, **1995**, 82, 123-128.
  19. Thomas, L. H.; Wales, C.; Zhao, L.; Wilson, C. C., Paracetamol Form II: An Elusive Polymorph through Facile Multicomponent Crystallization Routes, *Cryst. Growth Des.*, **2011**, 11, 1450–1452
  20. Lang, M.; Grzesiak, A. L.; Matzger, A. J., The Use of Polymer Heteronuclei for Crystalline Polymorph Selection, *J. Am. Chem. Soc.*, **2002**, 124, 14834–14835
  21. Vericat, C.; Vela, M. E.; Benitez, G.; Salvarezza, R. C., Self-assembled monolayers of thiols and dithiols on gold: new challenges for a well-known system, *Chem. Soc. Rev.*, **2010**, 39, 1805-1834
  22. Tai, Y.; Shaporenko, A.; Buck, M.; Eck, W.; Grunze, M.; Zharnikov, M., Fabrication of Thiol-Terminated Surfaces Using Aromatic Self-Assembled Monolayers, *J. Phys. Chem. B*, **2004**, 108, 16806–16810
  23. Wang, M.; Liechti, K. M.; Wang, Q.; White, J. M. Self-assembled silane monolayers: Fabrication with nanoscale uniformity, *Langmuir*, **2005**, 21, 1848–1857
  24. Granberg, R. A.; Rasmuson, A. C., Solubility of Paracetamol in Pure Solvents, *J. Chem. Eng. Data*, **1999**, 44, 1391–1395

25. Haisa, M., Kashino, S., Kawai, R., Maeda, H., The Monoclinic Form of p-Hydroxyacetanilide, *Acta Cryst.*, **1976**, 32, 1283-1285
26. Haisa, M., Kashino, S., Maeda, H., The Orthorhombic Form of p-Hydroxyacetanilide, *Acta Cryst.*, **1974**, 30, 2510-2512
27. Williams, D. B. G.; Lawton, M., Drying of Organic Solvents: Quantitative Evaluation of the Efficiency of Several Desiccants, *J. Org. Chem.*, **2010**, 75, 8351–8354
28. Nishi, N.; Hobara, D.; Yamamoto, M.; Kakiuchi, T., Chain-length-dependent change in the structure of self-assembled monolayers of n-alkanethiols on Au(111) probed by broad-bandwidth sum frequency generation spectroscopy *J. Chem. Phys.* **2003**, 118, 1904-1911.
29. Wenzl, I.; Yam, C. M.; Barriet, D.; Lee, T. R. Structure and Wettability of Methoxy-Terminated Self-Assembled Monolayers on Gold, *Langmuir* **2003**, 19, 10217-10224.
30. Lee, S.; Puck, A.; Graupe, M.; Colorado, R., Jr.; Shon, Y.-S.; Lee, T. R.; Perry, S. S. Structure, Wettability, and Frictional Properties of Phenyl-Terminated Self-Assembled Monolayers on Gold, *Langmuir* **2001**, 17, 7364.
31. Park, B.; Chandross, M.; Stevens, M. J.; Grest, G. S., Chemical Effects on the Adhesion and Friction between Alkanethiol Monolayers: Molecular Dynamics Simulations, *Langmuir* **2003**, 19, 9239-9245.
32. Mino, N.; Nakajima, K.; Ogawa, K., Control of Molecular Tilt Angles in Oriented Monolayers Deposited by a Chemical Adsorption Technique and Application of the Monolayers as an Alignment Film, *Langmuir* **1991**, 7, 1468-1472.



## Chapter 3. Conclusion and future works

### 3.1 Conclusion

The aim of this thesis is to develop SAM-functionalized substrates to study the role of different SAMs as heterogenous nucleation sites for polymorph control of a model pharmaceutical compound. In this work, I prepared 1-undecanethiol (UDT) and 11-mercapto-1-undecanol (MUOH) SAM chemistries on gold, and trichloro(octadecyl)silane (OTS), trichloro(octadecyl)silane (PTS) on silicon. Various solvent systems were then used to investigate their ability to influence the polymorph selection of a common drug, acetaminophen (ACM). In general, both the solvent and SAMs surface chemistry act in concert to control polymorph selection. Interestingly, the surface chemistry further influences the crystal orientation of the form II polymorph. This work raises additional questions about what happens at the early stage of the crystallization process and how solvent and substrate contribute to polymorphism control. Thus, more in-situ studies on the crystallization process should come next and, probably, by combining experimental data with computational crystal structure prediction (CSP), the nature of the solid form landscape would be viewed.

### 3.2 Preliminary blade-coating work

**Motivation.** From the last two years of work, I developed a reproducible system, in which SAMs are exploited to control nucleation, growth, and crystal polymorphs of acetaminophen. However, the mystery about what happens at the early stage of crystallization process and how solvent and substrate attribute to polymorphism

control, is still not well understood. Therefore, the structure evolution at the early stage of acetaminophen will be further studied by blade coating with in-situ grazing-incidence wide-angle X-ray scattering (GIWAXS) at Cornell's High Energy Synchrotron Source (CHESS). These studies will allow us to identify amorphous phases and polymorph formation at early times. Initial experiments were performed to validate this approach.

**Preparation.** SAMs-modified substrates and all solvent drying were prepared following the procedures described in Chapter 2. Doctor blade and little dipper were stored at Thurston 406.

**Substrate types and solvent types for blade coating.** Using a steel blade, none of the ACM solutions of water, ethanol, THF, 1,4-dioxane, and water/dioxane would form stable liquid-films on OTS SAMs when blade coating. While for blade coating on PTS SAMs, as shown in Tab. 1, ACM solutions of ethanol and 1,4-dioxane can be used to form liquid films. THF would also work only if an OTS-modified blade is used.

**Table 1.** Substrate types and solvent types for blade coating

<i><b>Solution</b></i>	<i><b>Thin liquid-film</b></i>
Water	No
Ethanol	Yes
THF	Yes (only with OTS modified blade)
1,4-dioxane	Yes
Water/1,4-dioxane	No

### **Blade-coating procedure**

- I. Clean doctor blade by acetone every time before use
- II. Fix SAM-modified substrate on the plate
- III. Adjust the height between substrate and blade
- IV. Move blade to the position right above SAM-covered area
- V. Drop ACM solution along the blade and make sure meniscus formed between blade and substrate
- VI. Do blade coating and wait for crystallization
- VII. Clean Doctor blade by acetone every time after use

## Preliminary results

**Table 2.** Preliminary results of manually blade coating

<i>Blade</i>	<i>Solvent</i>	<i>Solution Concentration</i>	<i>SAM chemistry</i>	<i>Temperature</i>	<i>Thickness</i>	<i>Polymorph</i>
steel	1,4-dioxane	15 mg/mL	PTS on silicon wafer	RT	2 layers of tape	monoclinic
steel	1,4-dioxane	15 mg/mL	PTS on silicon wafer	50 °C	2 layers of tape	monoclinic
steel	1,4-dioxane	15 mg/mL	PTS on silicon wafer	80 °C	2 layers of tape	monoclinic
steel	ethanol	100 mg/mL	PTS on silicon wafer	50 °C	2 layers of tape	monoclinic
OTS	THF	100 mg/mL	PTS on silicon wafer	RT	2 layers of tape	monoclinic
OTS	THF	100 mg/mL	PTS on silicon wafer	50 °C	2 layers of tape	monoclinic

**Manually blade coating.** I did blade coating experiments under different parameters as shown in Tab. 2 and, in those cases, I moved the blade manually, which means coating speed was not uniform. After blade coating, the solvent evaporated and the resulting crystal polymorph determined by XRD. Each type of experiment in Tab.2 was done only once.

**Table 3.** Preliminary results of blade coating with controlled speed

<i>Blade</i>	<i>Solvent</i>	<i>Solution Concentration</i>	<i>SAM chemistry</i>	<i>Temperature</i>	<i>Thickness</i>	<i>Polymorph</i>
steel	1,4-dioxane	15 mg/mL	PTS on silicon wafer	RT	76-102	monoclinic
steel	ethanol	15 mg/mL	PTS on silicon wafer	RT	76-102	orthorhombic
steel	1,4-dioxane	15 mg/mL	MUOH on gold	RT	76-102	orthorhombic
steel	ethanol	15 mg/mL	MUOH on gold	RT	76-102	orthorhombic

**Blade coating with controlled speed.** I also did blade coating experiments controlled by a “little dipper”. Experimental parameters and results are shown in Tab. 3. And coating speed was 300 steps per second. These films showed polymorph selectivity, which is promising for future experiments. Each type of experiments in Tab.2 was also done only once.

**Words for future students.** In my opinion, results in Tab. 3 are promising and should be a good start point, although those experiments were only done once before. However, there are still other parameters that you can play around with, such as temperature, thickness between substrate and blade, and coating speed. Thus, you would get a better understanding of how each parameter attributes to the crystallization results. Additionally, please feel free to ask me by email if there is anything else you need from me.